

Structural invariants of antigen binding: Comparison of immunoglobulin V_L - V_H and V_L - V_L domain dimers

(antibody/ β -sheet/electrostatics/strophoid/x-ray structure)

JIRÍ NOVOTNÝ AND EDGAR HABER

Molecular and Cellular Research Laboratory, Massachusetts General Hospital and Harvard Medical School, Boston, MA 02114

Communicated by Elkan R. Blout, March 11, 1985

ABSTRACT Antigen-combining site arises by noncovalent association of the variable domain of the immunoglobulin heavy chain (V_H) with that of the light chain (V_L). To analyze the invariant features of the binding region (V_L - V_H domain interface), we compared the known immunoglobulin three-dimensional structures by a variety of methods. The interface forms a close-packed, twisted, prism-shaped “ β -barrel” characterized by cross-sectional dimensions 1.04×0.66 nm and a top-to-bottom twist angle of 212° . The geometry of the interface is preserved via invariance of some 15 side chains, both inside the domains and on their surface. Buried polar residues form a conserved hydrogen-bonding network that has a similar topological connectivity in the two domain types; two hydrogen bonds contributed by invariant side chains extend across the interface and anchor the β -sheets in their relative orientation. Invariant aromatic residues close-pack at the bottom of the binding-site β -barrel with their ring planes oriented perpendicularly in the characteristic “herringbone” packing mode. Electrostatic computations that implicitly include solvent effects show the domains to be stabilized by large electrostatic forces. However, structures that were crystallized at lower pH have their electrostatic energies appropriately lowered, implying that full ionization of carboxyl side chains is essential for efficient electrostatic stabilization. The unusual mode of domain-domain association in the V_L - V_L dimer RHE correlates with its overall repulsive electrostatic energy (+54 kJ/mol), as opposed to negative (i.e., stabilizing) energy values (–263 to –543 kJ/mol) found in the domains of the other structures. The V_L - V_L dimer REI mimics closely the interface geometry of V_L - V_H dimers although its domain-domain contact area is lower by 18%.

The structural diversity of antibody molecules epitomizes one of the most interesting problems of molecular biology, that of a relationship between molecular shape and biological function. Although spatial structures of three different antibody binding sites have been elucidated (1–3), our knowledge of structural prerequisites of the antigen binding function remains incomplete. Relative importance of individual amino acid residues that form the antigen binding site is not well understood, nor is it clear how their presence influences antigen binding. Recent advances in genetic engineering have put at our disposal a means to modulate antibody specificity at will—e.g., by applying site-directed mutagenesis to genes encoding immunoglobulin polypeptide chains. This possibility, however, can only be realized on the basis of a sound understanding of principles that determine protein anatomy in general (4, 5) and that of antibody molecules in particular (6).

The antigen-combining site is formed by noncovalent association of two “variable” (V) domains provided by two

different polypeptide chains, heavy (H) and light (L). The V_L - V_H interface consists of two closely packed β -sheets and its geometry corresponds to a nine-stranded elliptical (4) or prism-shaped (7) barrel. The barrel forms the bottom and sides of the antigen binding site, and amino acid residues that are part of the domain-domain interface and appear not to be accessible to solvent or antigen contribute to antibody specificity (6).

Here we study those conformational features of the V_L and V_H domains that are conserved in all the antibodies and form the constant scaffold for the binding site. We do so by comparing three-dimensional structures with use of a novel procedure (8, 9): we superimpose, by the least-squares method, only those side chain atoms that are invariant in all the immunoglobulins. This allows for differences in functional importance of different parts of the structure and leads to more meaningful results than the method employed previously (10, 11), namely, a least-squares superposition of complete polypeptide chain backbones (i.e., optimization of structural correspondence over the domain as a whole). We also analyze the conserved hydrogen-bonding network existing among polar side chains that are buried inside the domains and discuss the contribution of electrostatic interactions to the stability of the binding site.

ATOMIC COORDINATES AND CALCULATIONS

Crystallographic coordinates of human Fab fragments NEW, KOL, and MCPC 603; V_L - V_L dimers RHE and REI; and Bence Jones protein (light-chain dimer) MCG were obtained from the Brookhaven Protein Data Bank (12). No attempts were made to energy-minimize or otherwise improve the original data. Structural manipulations, such as least-squares superpositions, generation of hydrogen bonded lists, potential energy evaluations, etc., were performed with the program CHARMM version 16 (13) as described (6, 14). The electrostatic potential was computed by use of a solvent-modified Coulomb formula (14). The effect of solvent was modeled by multiplying charges on atoms by a constant that depends linearly on the distance of the atom from the surface of the protein (15). The potential was evaluated to infinity; i.e., no distance cutoff was applied to evaluations of pairwise atomic interactions. Stereo drawings were made from CHARMM-generated files, using previously described graphics facilities and software (14). Amino acid alignments of immunoglobulin variable domains used as a basis for structural comparisons and residue numbering were those of Kabat *et al.* (16).

RESULTS AND DISCUSSION

Conservation of the Binding Site Geometry. Although all the immunoglobulin domains share the same folding scheme—two antiparallel β -sheets packed face-to-face (4)—the number of β -strands, strand orientation, side chain preponder-

The publication costs of this article were defrayed in part by page charge payment. This article must therefore be hereby marked “advertisement” in accordance with 18 U.S.C. §1734 solely to indicate this fact.

Abbreviations: V_L , light chain variable; V_H , heavy chain variable.

ance, and other structural characteristics differ widely among various domain types (V_L , V_H , and constant domains C_L , C_{H1} , C_{H2} and C_{H3}). Only three residues are common to all the domains: two cysteines that form a disulfide bridge between the β -sheets and a tryptophan that packs against them (17). Structural diversity of this kind correlates with the fact that different domain types perform different biological functions, such as antigen binding in V_H and V_L or complement binding in C_{H2} . Identical domain types, on the other hand, might be expected to have many more structural features in common.

To compare x-ray structures of V_L and V_H domains, the best-resolved crystallographic data-set, the Fab fragment KOL, was first chosen as a reference structure and oriented most conveniently in the reference frame of Cartesian coordinates ("barrel orientation" of figure 4 in ref. 6). Second, selected side chains of the V_L or V_H domains of Fab fragments NEW and MCPC 603 were superimposed, independently in each domain, on the corresponding side chains of the reference structure. Because of their invariance and central positions in the domain cores (17), residues Cys-23 and -88, Trp-35, and Phe-62 were chosen in the V_L domain; Cys-22 and -92, Trp-47, and Leu-78 were chosen in the V_H domain.

Fig. 1 displays the superimposed side chains and resulting polypeptide backbone fits of all the three V_L - V_H dimers. No attempt was made to reproduce the exact mode of domain-domain association with our matching procedure, yet polypeptide chain segments involved in the V_L - V_H interface can be seen to overlay virtually exactly (the average root-mean-square difference of these segments among the three structures compared is 0.11 nm). At the same time, significant differences are apparent in backbone conformations of solvent-facing sides of the dimer (root-mean-square differences of 0.5 nm and more). The close match of segments forming the V_L - V_H interface was striking and suggested that despite amino acid variability of both the variable domains (68% of positions vary in the three V_L domains, and 74% in the V_H domains), side chains are conserved in various regions of V_L and V_H primary structures in such a way as to preserve the geometry of the V_L - V_H interface (the antigen-combining region).

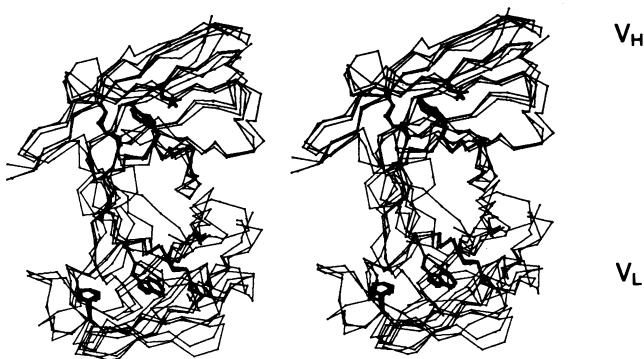


FIG. 1. Superposition of KOL, MCPC 603, and NEW V_L and V_H domains. Using the program CHARMM, 4 side chains in each domain were least-squares superimposed on the corresponding side chains from the domain of the reference structure (KOL). The side chains, shown in heavy lines, are the invariant residues Cys-23 and -88, Trp-35, and Phe-62 in the V_L domains and Cys-22 and -92, Trp-36, and Leu-78 in the V_H domains. Polypeptide backbones (light lines) are traced by C^α atoms. Note that polypeptide chain segments involved in the V_L - V_H interface (antigen-combining region) overlay virtually exactly (root-mean-square shift 0.11 nm) despite the fact that the V_L and V_H domains were matched independently and no attempt was made to reproduce the exact mode of domain-domain association.

Importance of Exposed Nonpolar and Buried Polar Residues. Naturally, the question arises how conservation of side chains in separate domains gives rise to the invariance of the domain-domain interface.

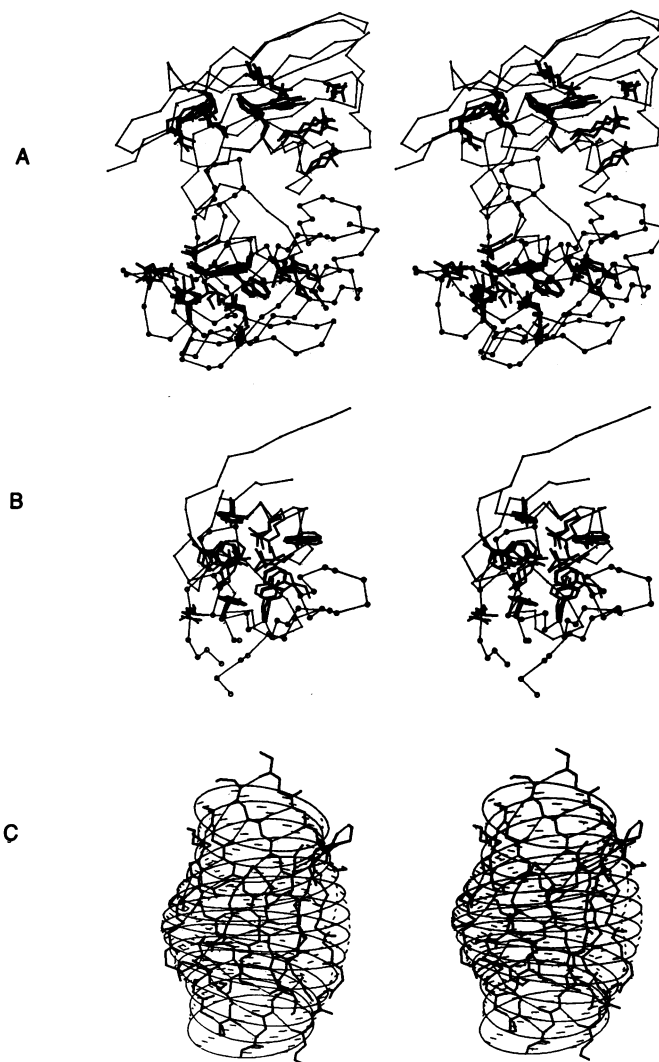


FIG. 2. Conserved features of the antigen-combining region (V_L - V_H domain interface). (A) Comparison of selected invariant side chains in superimposed KOL, MCPC 603, and NEW V_L and V_H domains. The figure shows C^α plot of a polypeptide backbone of the reference structure (V_L - V_H dimer KOL, V_L domain α -carbons represented by circles) together with selected side chains of all three V_L - V_H dimers. In addition to the residues used to produce the least-squares fit (see Fig. 1 and legend), the side chains that superimpose virtually exactly are Gln-6, Val-19, Gln-37, Leu-47, Ile-48, Leu-73, Glu-81, Asp-82, Tyr-86, and Thr-102 in the V_L domains and Leu-4, Gln-6, Leu-20, Phe-29, Arg-38, Glu-46, Asp-86, and Tyr-90 in the V_H domains. (B) A close-up of the antigen-combining region (V_L - V_H interface) showing positions of invariant residues that mediate domain-domain interaction. The interface-forming polypeptide chain segments of KOL are drawn in light lines (V_L domain with circles). Residues shown from the three structures (heavy lines) were not mutually superimposed; rather, the fit was produced as described in the legend to Fig. 1. Note the six aromatic rings in the interface (Tyr-36, Tyr-87, and Phe-98 of V_L and Trp-47, Tyr-91, and Trp-103 of V_H). The two forked side chains at the bottom of the binding site β -barrel are glutamine residues 38 (V_L) and 39 (V_H) involved in interdomain hydrogen bonds. (C) A detailed view of KOL backbone segments that form the interface β -barrel (binding site). Heavy line, β -strands forming the barrel; light line, interstrand hydrogen-bonds and the least-squares-fitted strophoid surface that was used to obtain the dimensions of the barrel (see Table 1 for β -barrel dimensions).

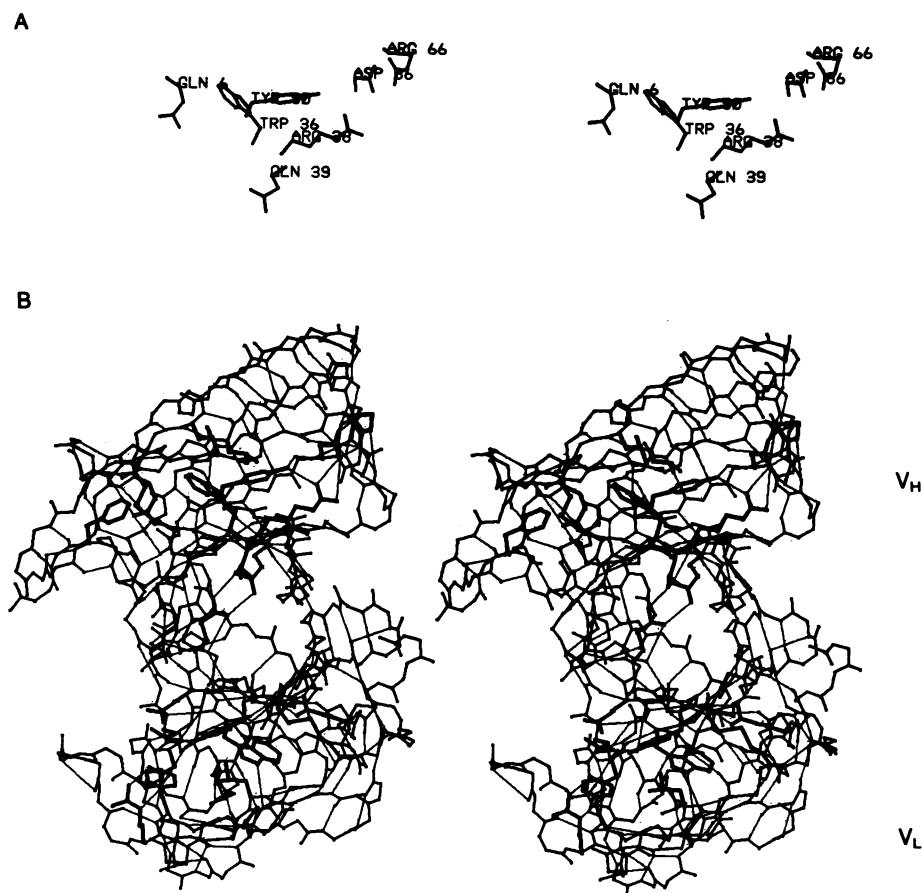


FIG. 3. The conserved hydrogen-bonding pattern provided by polar residues buried inside the V_L and V_H domains of KOL. (A) To facilitate orientation, prominent side chains are displayed and identified by names and numbers in the same orientation as in B. (B) Polypeptide chain backbones of both domains are denoted by heavy lines, and hydrogen bonds by light lines. In addition to the regular interbackbone hydrogen-bonding network characteristic of antiparallel β -sheets, there are hydrogen bonds provided by side-chain atoms. Note the two hydrogen bonds of Gln-38 (V_L) and Gln-39 (V_H) that span the domain-domain interface.

Amino acid alignments show that there are 37 residues conserved among the KOL, NEW, and MCPC 603 V_L domains and 31 residues among the V_H domains. They include the side chains used to produce the least-squares fit, and they always occur at positions invariant in many other V_L and V_H domains (16). The majority of them have hydrophobic side chains, and our solvent-accessibility calculations (18, 19) confirm the previous observation (20) that virtually all of them are buried inside the domains. However, we found that

some of the nonpolar residues are exposed to solvent, while some of the polar ones are buried. The structural importance of the exposed nonpolar and buried polar residues is apparent from the fact that they belong to the most stringently conserved side chains in both V_L and V_H domains (16). The solvent-exposed residues are Tyr-36, Leu-46, Tyr-87, and Phe-98 in the V_L domain and Val-2, Leu-45, Trp-47, and Trp-103 in the V_H domain; the buried residues are Gln-6, Gln-37, Asp-82, and Thr-102 in the V_L domain and Gln-6,

Table 1. Geometry of domain-domain interfaces (antigen-combining sites)

Structure	Major semiaxis, nm	Minor semiaxis, nm	Helical pitch, nm	Twist angle (top to bottom)	Goodness of fit*
KOL V_L - V_H	1.013	0.652	4.195	214°	0.140
MCPC 603 V_L - V_H	1.081	0.662	4.245	220°	0.132
NEW V_L - V_H	1.073	0.630	4.333	210°	0.150
REI V_L - V_L	0.994	0.688	4.270	204°	0.124
Average	1.04 ± 0.04	0.66 ± 0.02	4.26 ± 0.05	212° ± 6°	
MCG V_L - V_L †	0.904	0.747	6.223	139°	0.144

It was shown (28) that the geometry of β -sheet- β -sheet interfaces can be approximated by strophoid (twisted hyperboloid) surfaces. The strophoid model gives a significantly better goodness of fit than the cylindrical model of V_L - V_H β -sheet interface (6). The values [nm] were obtained by least-squares fitting of strophoids into polypeptide chain backbones of interface-forming V_L and V_H β -sheets. The surface is mathematically defined by the following four parameters: major and minor semiaxis of (elliptical) cross-section, surface curvature (analogous to the curvature of the hyperboloid), and pitch of the twist (the smaller the pitch, the more twist there is to the surface).

*Root-mean-square difference between the least-squares-fitted strophoid surface and the backbone atoms N, C α , and C.

†Only α -carbon atom coordinates are available for this structure. Consequently, the values obtained are not directly comparable to those obtained for the other structures.

Arg-38 (Lys-38), and Asp-86 in the V_H domain. Figs. 2 and 3 show that (i) conformations of these side chains are identical, within the limits of crystallographic resolution, in all the structures compared; (ii) all the conserved, solvent-exposed hydrophobic side chains are involved in domain-domain association at the bottom of the binding-site barrel and become buried upon formation of the V_L - V_H dimer; and (iii) the buried polar residues are engaged in a conserved hydrogen-bonding network that spans both β -sheets of one domain and tethers such distant parts of the structure as backbone positions 6 and 86. Two hydrogen bonds formed between Gln-38 of V_L and Gln-39 of V_H extend the hydrogen-bonded network across the domain-domain interface and anchor the interface β -sheets in their relative orientation. We propose that all these structural features contribute to invariance of the binding site geometry.

Two-Fold Symmetry of the Binding Site. Figs. 2 and 3 make it apparent that important side chains are related in the V_L - V_H dimer by a pseudo-dyad that is approximately coincident with the axis of the interface β -barrel (21-23). Thanks to this symmetry, Bence Jones proteins (V_L - V_L dimers) are able to associate in the same manner as the V_L - V_H module, creating a domain interface that structurally resembles the antigen-combining site (24, 25) and possesses antigen-binding capacity (26, 27). In fact, cross-sectional dimensions of V_L - V_L interfaces in crystallographic structures REI and MCG correspond closely to those of V_L - V_H domain dimers (Table 1). Side chains at the REI V_L - V_L interface, particularly the pair Gln-38/Gln-38 and the aromatic rings, mimic the side chain arrangement of the KOL V_L - V_H interface (Fig. 4). Solvent accessibility calculations show that surface area buried upon REI V_L - V_L dimerization is smaller by some 3.35 nm² than the average V_L - V_H contact area. However, several strong, buried hydrogen bonds provided by residues from hypervariable loops and extending across the V_L - V_L interface supply an additional stabilization in the REI domain dimer (24).

Aromatic Side Chains at the Bottom of the Site. Fig. 2B illustrates the close-packed cluster of the invariant aromatic side chains at the V_L - V_H interface. The clustering is similar to that of other "herringbone" packing motifs (29), characterized by ring centroid distances of approximately 0.56 nm and ring dihedral angles close to 60° (30). Such "perpendicular" ring arrangement is also found in benzene crystals (31). The herringbone geometry principally differs from an apparently directionless packing of aliphatic side chains found at typical β -sheet interfaces (7, 32), and its static and dynamic aspects might be of importance to the process of antigen binding. Numerous experimental data point to small but definite structural rearrangements of antibody molecules upon antigen binding (33-37), and recent crystallographic studies of aromatic ligands bound to the V_L - V_L dimer MCG

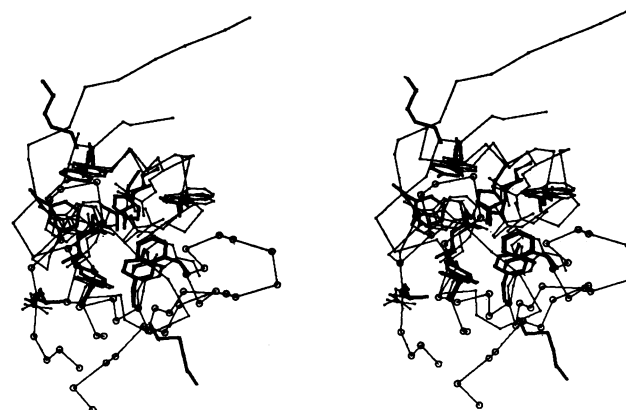


FIG. 4. A close-up of the side-chain arrangement at the V_L - V_L interface of REI. To emphasize the similarity to V_L - V_H interfaces, the backbone segments of KOL that form its binding site are drawn in light lines, together with the prominent side chains that mediate domain-domain contacts between KOL V_L - V_H domains (see also Fig. 2B). The selected domain-domain contacting residues of REI are drawn in heavy lines.

detected rearrangements of aromatic side chains within the binding site β -barrel (38).

Electrostatic Interactions in Variable Domains and Fv Fragments. In computing the electrostatic energy on atoms, residues, and whole domains, we used two different approaches: (i) the model of electrostatics that incorporates an approximate representation of solvent effects (14) and (ii) the unmodified Coulomb formula with the dielectric constant = 50, evaluated to infinity (39). Both methods yielded comparable results and only the solvent-modified energies are reported here. Table 2 shows that the isolated V_L and V_H domains are generally stabilized by electrostatic contributions regardless of their net charge, $\sum q_i$ (q_i , the charge of the i th side chain, is +1 for lysine and arginine and is -1 for aspartate and glutamate). However, full ionization of acidic side chains is essential for efficient electrostatic stabilization, since the electrostatic energy of structures that were crystallized at lower pH is lower.

The total electrostatic energy of the domains represents a balance between attractive and repulsive side chain interactions. Some of these contributions were found to be very large compared to the resulting total energy; the energy of a single residue, expressed as kJ/residue, may often amount to 20-30% of the total electrostatic energy of the domain (kJ/mol). Residues contributing most significantly are Lys-45, Arg-61, Lys-103, Glu-81, and Asp-82 in the V_L domains and Arg-38, Lys-43, Glu-85, and Asp-86 in the V_H domains. All of them are conserved in other immunoglobulins as well (16) although Arg-38 of V_H is often replaced by a lysine.

Table 2. Electrostatic energy (kJ/mol) and crystallization conditions of immunoglobulin Fv fragments

Structure	Net charge of domain dimer	Electrostatic potential					Mother liquor	
		V_L		V_H		V_L - V_H dimer, total	pH	(NH ₄) ₂ SO ₄ , % saturation
		Isolated	In dimer	Isolated	In dimer			
KOL	-4	-209	-201	-326	-305	-510	8.0	18
REI*	0	(-180)					8.0	22
MCPC 603	+3	-251	-238	-313	-305	-543	7.0	42
NEW	+4	-58	-125	-125	-155	-263	5.0	42
RHE	-12	-38	+21	-38†	+29†	+54	4.5	26

Crystallization conditions were as described for KOL (46), REI (40), MCPC 603 (41), NEW (42), and RHE (43).

*Since the crystallographic resolution does not permit one to distinguish side-chain amide nitrogens and oxygens in the REI V_L - V_L dimer, its exact electrostatic potential could not be determined. The value given represents an estimate based on arbitrarily assigned amide atoms.

†RHE is a Bence-Jones-type V_L - V_L dimer, not a V_L - V_H heterodimer; the values given in the V_H column refer to the other V_L domain of the V_L - V_L module.

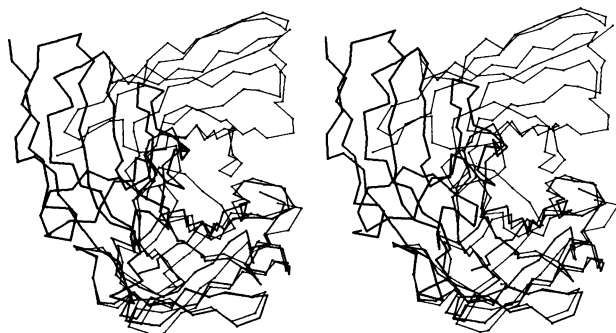


FIG. 5. The mode of V_L - V_L association in RHE. C^α atoms of polypeptide chain backbones are plotted. The four invariant side chains of the first V_L domain of RHE (medium line) were least-squares superimposed on the V_L domain of KOL (light line) as described in the legend to Fig. 1. The second V_L domain of RHE (heavy line) is not matched by this procedure with the KOL V_H domain, as expected if the domain-domain association mode in RHE is comparable to that of V_L - V_H dimers. Rather, the second V_L domain is displaced far to the left of the V_H domain. Electrostatic interaction in the RHE V_L - V_L dimer is repulsive (Table 2), indicating that this dimerization mode might be an artifact of the low pH (4.5) used to crystallize the RHE V_L - V_L dimer.

Lys-45 of V_L and Arg-35 and Lys-48 of V_H belong to those polypeptide chain segments that are directly involved in the binding site. In this sense, the electrostatic stabilization appears to be an indispensable part of the binding site architecture.

Unusual Mode of V_L - V_L Association in RHE. The importance of electrostatic interactions to the integrity of the binding site is next discussed for the structure RHE (44, 45). The two V_L domains of this structure do not dimerize "face to face" as in the V_L - V_H modules but "side by side" (Fig. 5), violating virtually all the characteristics of domain-domain association described above. No close-packed, β -barrel structure exists at the domain-domain interface; instead, the β -hairpin loop of residues 38-48 is displaced some 0.4 nm away from its usual position and makes two interdomain, backbone-to-backbone hydrogen bonds as in regular antiparallel β -sheets. In an apparent correspondence with this anomalous dimerization mode, electrostatic stabilization of the RHE V_L domains is only a fraction of that seen in, e.g., KOL or MCPC 603 domains (Table 2). It would thus appear that a close V_L - V_L association of RHE is only possible under the particular crystallization conditions of extreme hydrogen ion concentration (pH 4.5), where electrostatic interactions are reduced to a small fraction of their original strength and do not significantly enter into the total energetic balance of Gibbs free energy of domain folding and domain-domain association. However, small crystals of RHE were also obtained at pH 6 and their diffraction pattern was reported to be identical to those of the bigger crystals obtained at pH 4.5 (43). Further computational and crystallographic study is needed to clarify the influence of electrostatic force on stability of variable domains and V_L - V_L or V_L - V_H dimers.

We thank Drs. D. Davies (National Institutes of Health), B. C. Wang (Veterans' Administration Medical Center, Pittsburgh), and R. Huber (Max-Planck-Institut, Martinsried by München, F.R.G.) for making crystallographic coordinates available to us prior to their public release. We are indebted to Prof. M. Karplus (Harvard University, Cambridge, MA) for insightful criticism and helpful

comments, Dr. Robert Brucoleri (Massachusetts General Hospital) for many helpful suggestions, and Dr. William Furey (Veterans' Administration Medical Center, Pittsburgh) for discussions. This work was made possible by the generous support of J. Newell, head of the Cardiac Computer Center at Massachusetts General Hospital.

- Marquart, M., Deisenhofer, J. & Huber, R. (1980) *J. Mol. Biol.* **141**, 369-391.
- Saul, F. A., Amzel, L. M. & Poljak, R. J. (1978) *J. Biol. Chem.* **253**, 585-597.
- Segal, D., Padlan, E. A., Cohen, G. H., Rudikoff, S., Potter, M. & Davies, D. (1974) *Proc. Natl. Acad. Sci. USA* **71**, 4298-4302.
- Richardson, J. S. (1981) *Adv. Protein Chem.* **34**, 167-339.
- Chothia, C. (1984) *Annu. Rev. Biochem.* **53**, 537-572.
- Novotný, J., Brucoleri, R., Newell, J., Murphy, D., Haber, E. & Karplus, M. (1983) *J. Biol. Chem.* **258**, 14433-14437.
- Chothia, C. & Janin, J. (1981) *Proc. Natl. Acad. Sci. USA* **78**, 4146-4150.
- Chothia, C. & Lesk, A. M. (1982) *J. Mol. Biol.* **160**, 309-323.
- Kabsch, W. (1976) *Acta Crystallogr. Sect. A* **32**, 922-923.
- Padlan, E. A. & Davies, D. (1975) *Proc. Natl. Acad. Sci. USA* **72**, 819-823.
- Amzel, L. M. & Poljak, R. J. (1979) *Annu. Rev. Biochem.* **48**, 961-997.
- Bernstein, F. C., Koetzle, T. F., Williams, G. J. B., Meyer, E. F., Brice, M. D., Rodgers, J. R., Kennard, O., Shimanouchi, T. & Tasumi, M. (1977) *J. Mol. Biol.* **112**, 535-542.
- Brooks, B., Brucoleri, R., Olafson, B. D., States, D. J., Swaminathan, S. & Karplus, M. (1983) *J. Comput. Chem.* **4**, 187-217.
- Novotný, J., Brucoleri, R. & Karplus, M. (1984) *J. Mol. Biol.* **177**, 787-818.
- Northrup, S. H., Pear, M. R., Morgan, J. D., McCammon, J. A. & Karplus, M. (1981) *J. Mol. Biol.* **153**, 1087-1109.
- Kabat, E. A., Wu, T. T., Bilofsky, H., Reid-Miller, M. & Perry, H. (1983) *Sequences of Proteins of Immunological Interest* (National Institutes of Health, Bethesda, MD).
- Lesk, A. & Chothia, C. (1982) *J. Mol. Biol.* **160**, 325-342.
- Lee, B. K. & Richards, F. M. (1971) *J. Mol. Biol.* **55**, 379-400.
- Richmond, T. J. & Richards, F. M. (1978) *J. Mol. Biol.* **119**, 537-555.
- Padlan, E. A. (1979) *Mol. Immunol.* **16**, 287-296.
- Davies, D. R., Padlan, E. A. & Segal, D. (1976) *Annu. Rev. Biochem.* **44**, 639-667.
- Padlan, E. A. (1977) *Q. Rev. Biophys.* **10**, 35-65.
- Davies, D. R. & Metzger, H. (1983) *Annu. Rev. Immunol.* **1**, 81-117.
- Epp, O., Colman, P., Feilhammer, H., Bode, W., Schiffer, M. & Huber, R. (1974) *Eur. J. Biochem.* **45**, 513-524.
- Schiffer, M., Girling, R. L., Ely, K. R. & Edmundson, A. B. (1973) *Biochemistry* **12**, 1620-1631.
- Edmundson, A. B., Ely, K. R., Girling, R. L., Abola, E. E., Schiffer, M., Westholm, F. A., Fausch, M. D. & Deutsch, H. F. (1974) *Biochemistry* **13**, 3816-3827.
- Schechter, I., Ziv, E. & Licht, A. (1976) *Biochemistry* **15**, 2785-2790.
- Novotný, J., Brucoleri, R. & Newell, J. (1984) *J. Mol. Biol.* **177**, 567-573.
- Nockolds, C. E., Kretsinger, R. H., Coffee, C. J. & Bradshaw, R. A. (1972) *Proc. Natl. Acad. Sci. USA* **69**, 581-584.
- Burley, S. K. & Petsko, G. A. (1985) *Science*, in press.
- Wyckoff, R. W. G. (1969) *Crystal Structures* (Wiley, New York), 2nd Ed., Vol. 6, Part I, pp. 1-2.
- Cohen, F. E., Sternberg, M. J. E. & Taylor, W. R. (1981) *J. Mol. Biol.* **148**, 253-272.
- Holowka, D. A., Strosberg, A. D., Kimball, J. W., Haber, E. & Cathou, R. E. (1972) *Proc. Natl. Acad. Sci. USA* **69**, 3399-3403.
- Lancet, D. & Pecht, I. (1976) *Proc. Natl. Acad. Sci. USA* **73**, 3549-3553.
- Levison, S. A., Hicks, A. N., Portman, A. J. & Dandliker, W. B. (1975) *Biochemistry* **14**, 3778-3786.
- Schlessinger, J., Steinberg, I. Z., Givol, I. D., Hochman, J. & Pecht, I. (1975) *Proc. Natl. Acad. Sci. USA* **72**, 2775-2779.
- Zidovetzki, R., Blatt, Y. & Pecht, I. (1981) *Biochemistry* **20**, 5011-5018.
- Edmundson, A. B., Ely, K. R. & Hurren, J. N. (1984) *Mol. Immunol.* **21**, 561-576.
- Warshel, A., Russell, S. T. & Churg, A. K. (1984) *Proc. Natl. Acad. Sci. USA* **81**, 4785-4789.
- Palm, W. (1970) *FEBS Lett.* **10**, 46-48.
- Rudikoff, S., Potter, M., Segal, D. M., Padlan, E. A. & Davies, D. R. (1972) *Proc. Natl. Acad. Sci. USA* **69**, 3689-3692.
- Rossi, G., Choi, T. K. & Nisonoff, A. (1969) *Nature (London)* **223**, 837-838.
- Wang, B. C. & Sax, M. (1974) *J. Mol. Biol.* **87**, 505-508.
- Furey, W., Wang, B. C., Yoo, C. S. & Sax, M. (1983) *J. Mol. Biol.* **167**, 661-692.
- Wang, B. C., Yoo, C. S. & Sax, M. (1979) *J. Mol. Biol.* **129**, 657-674.
- Palm, W. (1976) *Hoppe-Seyler's Z. Physiol. Chem.* **357**, 799-812.